Applications of Silicon Detectors

Hartmut F.-W. Sadrozinski

***Abstract*—The principle of operations and the development and applications of silicon detectors are discussed. The application of strip detectors in high-energy physics follows Moore's law in both the area and the channel count. New developments include pixel and drift detectors. Examples of use in space sciences and the growing use in medical applications are given. The role of silicon detectors in the detection of photons is explained. Frequent reference will be made to papers submitted to the IEEE2000 NSS-MIC.**

***Index Terms*—Applications in astrophysics, applications in medical sciences, applications in particle physics, pixel detectors, silicon, silicon gamma detectors, silicon photon detectors, silicon strip detectors, tracking detectors.**

I. Introduction

SILICON detectors have found use in many fields of physical research. Their application extends from the interactions of leptons, quarks, gluons, gauge bosons, and the hunt for the Higgs particles at the scale of $<10^{-20}$ m to investigations of large scales ($>10^{28}$ m) of the entire universe. In between these extremes, they are used in nuclear physics, crystallography, and medicine for imaging and mechanical engineering for alignment. In each of the many applications, they have been modified to fit the energy scale, time structure, and signal characteristics of the application.

In the following, the principle of operation of the silicon detector will be explained briefly. Then the development of silicon strip detectors as tracking detectors in high-energy physics (HEP) will be traced. With the help of typical examples of the application in HEP, astrophysics, and medicine the development and change of the silicon strip detector paradigm will be followed. The development of pixel detectors will be surveyed. The detection of photons in medicine and astrophysics with silicon detectors will be explained.

II. Principle of Operations of Silicon Detectors

One of the primary reasons for the common use of silicon as detector material is that it is a semiconductor [1] with a moderate bandgap of 1.12 eV. This is to be compared to the thermal energy at room temperature of $kT = 1/40$ eV. Thus cooling is needed only in ultra-low-noise applications or when required to mitigate radiation damage [2], [3]. The energy to create an electron-hole pair is 3.6 eV, compared to the ionization energy of 15 eV in argon gas, leading to an ionization yield for minimum ionizing particles (MIPs) of about 80 electron-hole (e-h) pairs per micrometer. Thus about 23 000 e-h pairs are produced in the customary wafers thickness of 300 μm and collected in about 30 ns without a gain stage.

The wafers are normally n-type with a high resistivity of about 5 kΩ-cm, and with a low-resistivity p-implant, in the form of pads, strips, or pixels, to create a junction. With a reverse bias of less than 100 V, the detectors can then be fully depleted such that only the thermally generated current contributes to the leakage current. Larger thickness requires much higher voltage because the depletion voltage increases with the square of the thickness.

The area of the detectors is limited to the standard wafer sizes used in high-resistivity processing by industry, which has increased the wafer size from 4 to 6 inches in the last two years. Larger area detectors are now routinely made by assembling and wire bonding several detectors into so-called ladders, with fairly long readout strips.

Searches for a different material that could replace silicon as the semiconductor of choice in tracking devices have not been successful [4], [5]. One reason for the uniqueness of silicon is its wide technology base [application-specific integrated circuits (ASICs), diodes, and detectors], and it has helped to spawn the use of pixel detectors [hybrids, charge-coupled devices (CCDs), CMOS detectors] for truly two-dimensional (2-D) applications.

Simulations have played an important role in the development of silicon detectors. They cover processing details [6], optimization of the geometry [7], [8], and limiting the breakdown [9].

III. Charged Particle Tracking

The detection of charged particles is based on the specific energy loss in matter. The signal is proportional to the specific energy loss ("stopping power") and the thickness of the detector. Fig. 1 shows the energy loss dE/dx in Si for muons and electrons as a function of particle momentum p [10]–[12]. In these units and as a function of $\beta * \gamma$, the curve is approximately universal for all materials for particles with the same charge, up to high energy, where radiation takes over. Three regions are worth emphasizing:

1) the low energy range with $0.05 < \beta * \gamma < 1$, where the energy loss is proportional to $1/p^2$, and thus can be used to measure the particle momentum;
2) the region of minimum ionization with $1 < \beta * \gamma < 100$, where an MIP deposits about 1.5 MeV/(g/cm^2);
3) the radiation region $\beta * \gamma > 5000$, where most of the energy loss occurs via radiation.

The useful thickness of the silicon detectors is bracketed on one hand by the desire for large signals, which calls for thick detectors, and on the other hand by the desire to keep the depletion voltage low and by the need to limit the effect of multiple scattering of the particle. While passing through material,

Manuscript received November 23, 2000; revised March 7, 2001 and March 22, 2001. This work was supported in part by the U.S. Department of Energy.

The author is with the Santa Cruz Institute for Particle Physics (SCIPP), University of California, Santa Cruz, CA 95064 USA (e-mail: hartmut@scipp.ucsc.edu).

Publisher Item Identifier S 0018-9499(01)06957-X.

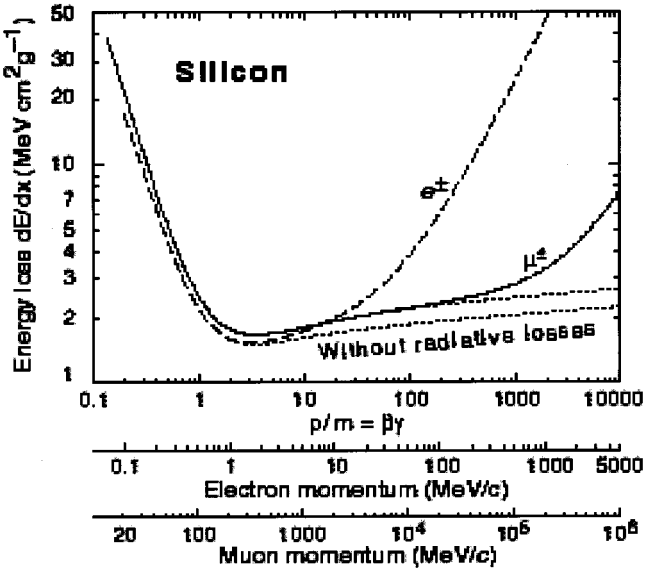

Fig. 1. Energy loss ("stopping power") of muons and electrons in Si. This curve is universal for all particles as a function of $\beta * \gamma$ until, at high enough energies, radiation takes over. At low energies, the momentum of the particle can be determined from the energy loss [10]–[12].

the particle will undergo multiple Coulomb interactions, which result in a deflection from the original direction. The multiple scattering angle θ_o depends linearly on the inverse of the momentum p and on the square root of the material thickness t in units of a material constant, the radiation length X_o

$$\theta_o \approx \frac{(13.6\ \text{MeV})}{\beta \cdot p} \cdot \sqrt{t/X_o}. \tag{1}$$

Thus, either very thin detectors or high-energy particles (or both) are required to allow good position resolution. The typical silicon detector thickness of 300 μm amounts to 0.3%X_o.

How well the tracking detector performs depends mostly on the signal-to-noise ratio (SNR). It determines how many false hits are accepted and if superior position accuracy due to charge sharing can be achieved. As mentioned, the signal depends on the detector thickness, and the noise more or less on the area of the detector element and on the shaping time. Thus detectors with small area readout sections can provide good performance even if the signal is generated only in a thin active volume. Detectors with large area readout sections can achieve good signal-to-noise with long shaping times.

IV. The Rise of Silicon Strip Detectors

Silicon detectors have been used and are still in use in low-energy spectroscopy [13], [14], due in part to the large e-h yield and low leakage currents. The use of silicon strip detectors in HEP particle tracking got a boost from the introduction of the planar technology by Kemmer [15], with fixed target experiments at both CERN [16] and FNAL [17]. Fig. 2 shows the setup of the experiment E706: the detectors of the dimensions 5×5 cm^2 are dwarfed by the fanouts, which are needed to bring the signals to the large banks of amplifier boards with discrete components [17].

The next step forward came through the development of ASIC amplifier chips of the size that they could be coupled

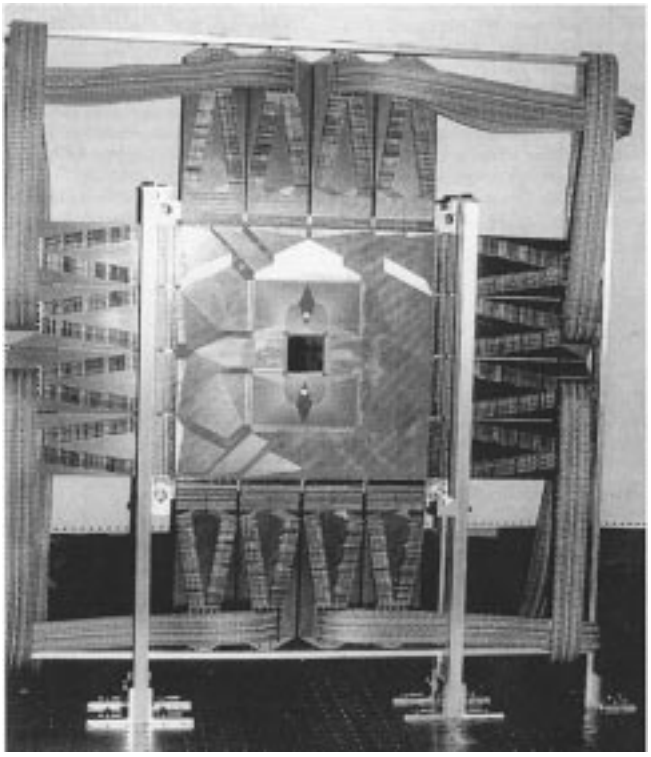

Fig. 2. The early years: experimental setup with silicon strip detectors in a fixed target experiment (E706 at FNAL). The 5×5 cm^2 silicon detectors are seen in the center, with the fanout cables and amplifier banks dominating the picture. From [17].

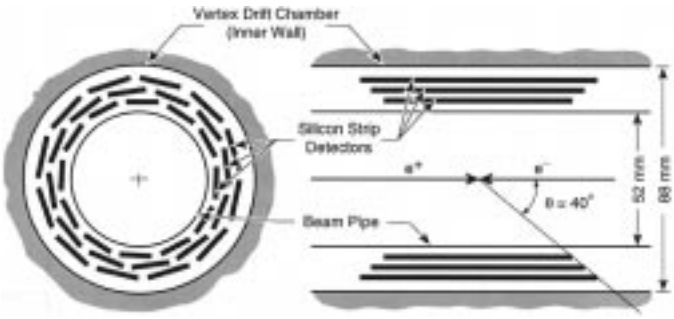

Fig. 3. Vertex detector paradigm embodied in the Mark2 silicon vertex detector: The inner radius is only 2.5 cm, the ASICs (not shown) are at the end of the ladders outside the tracking volume, and the detectors are very thin. From [19].

directly to the detectors [18]. In the silicon detector developed for the Mark2 [19] at the SLAC Linear Collider (SLC), shown in Fig. 3, the vertexing errors due to multiple scattering were reduced by the following *paradigm for vertex detectors*:

1) ASICs at the end of 'ladders";
2) minimize the mass inside the tracking volume;
3) minimize distance between interaction point and detectors.

Vertex detectors enabled a new area of heavy flavor physics both in fixed target and colliding beam experiments. For example, all four LEP experiments had vertex detectors using silicon strip detectors [20]. The next step came in the use of radiation-hard electronics [21], and the realization that high luminosity experimentation will require special attention to radiation

damage effects (see [2] and [3] for details). Still following the vertex detector paradigm are the vertex detectors for the B-factory detectors, Belle [22] and Babar [23]. The colliding beams have different energies, such that the center-of-mass is moving, allowing the determination of asymmetries between the decay times of particle and antiparticle. The presence of many low-energy particles in the decays requires that the detectors present the minimum amount of material in the active volume.

Silicon strip detectors have been introduced into space sciences, following their successful use as tracking detectors in accelerator experiments. A large tracking system in a magnetic field has been developed for AMS [24], still following the vertex paradigm to minimize the mass inside the tracking volume. This accounts for the extremely long ladders of 65 cm.

A shift in paradigm occurred with the development of tracking detectors for hadron colliders. Starting with CDF and D0 [25], the new emphasis is not only on vertexing but also on full tracking, including momentum determination in the magnetic field. The detectors become so large that the electronics, cables, and cooling cannot be kept outside the active volume but are an integral part of the detector modules. This paradigm shift from vertex detector to inner tracking detector is continuing in the LHC detectors ATLAS [26] and CMS [27], where the accumulated material in the inner detector reaches the order of a full radiation length in large parts of the detectors. That these detector systems exhibit satisfactory performance with that much material in the active volume is only possible because of the increased energy of the particles.

The *new paradigm for inner trackers* is:

1) cover a large area with many layers;
2) detector modules including ASICs and services inside the tracking volume;
3) module size limited by electronic noise due to fast shaping time of electronics.

With CMS, the silicon strip detectors have arrived: the entire inner tracking system up to a radius of 1.1 m will be built with silicon detectors, with a total silicon area of 230 m^2 and about 10 million readout channels. The overriding issues at the LHC are radiation hardness, which has to be mitigated by cooling; and quality assurance, requiring detailed studies of the detector performance before and after irradiation [28].

The development of the silicon strip detectors follows a version of Moore's law[1] [29], which implies exponential growth as a function of time. This is true for the detector area, shown in Fig. 4, and in the number of electronics channels used, shown in Fig. 5.

The difference between ground- and space-based application is evident in Fig. 6, where the silicon area is shown for the number of electronics channels needed: the space-based detectors (full symbols) are overcoming the limited resources (mainly power) in space by employing a fairly large detector, either with very long readout channels or coarse pitch, and fewer electronics channels.

Even the cost of silicon strip detectors follows Moore's law, but now with a negative slope. Since the first commercial detectors, the price per detector area has dropped by a factor of about 40. This was made possible by a number of factors:

[1]See http://mason.gmu.edu/~rschalle/moorelaw.html#N_7_

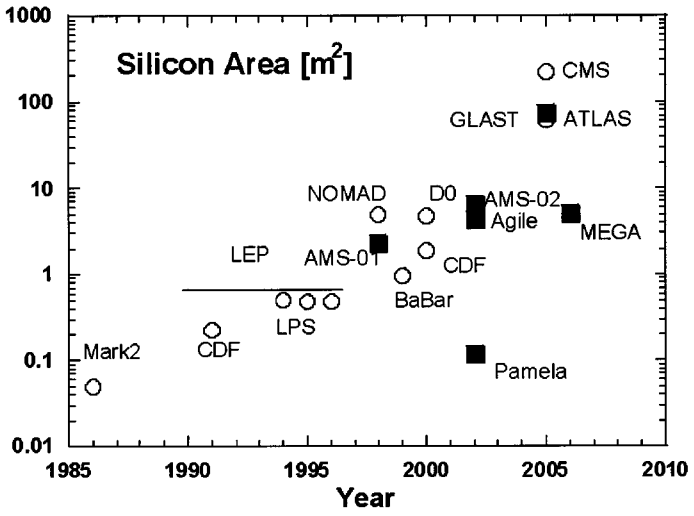

Fig. 4. The rise of the silicon detector: area of silicon detectors in experiments as a function of time. The full squares denote space-based instruments. The exponential growth of the area with time is an expression of Moore's law.

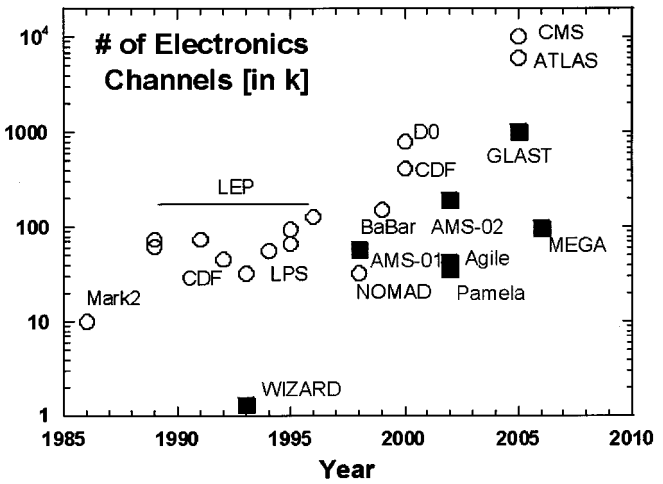

Fig. 5. The rise of the silicon detector: number of electronics channel of silicon detectors in experiments as a function of time. The full squares denote space-based instruments. The exponential growth of the number of channels with time is an example of a "Moore's plot."

1) the wafer area increased by changing from 4- to 6-in wafers;
2) the wafer area is being utilized better by designing the detectors to be square;
3) the cost of wafer processing was reduced by a factor of four, partly due to the much larger orders;
4) a close collaboration between industry and experimenters is bearing fruit.

The price for an ac-coupled detector is now only five times the cost of the blank high-resistivity wafer. At the same time, the quality of the detectors improved steadily: e.g., GLAST detectors [30] show a leakage current of less than 2 nA/cm^2, with the fraction of bad channels $<2 * 10^{-4}$.

V. Pixel Detectors

Two-dimensional information is needed for most tracking application. Depending on the particle density, different approaches can supply the 2-D information. For low particle

density, projective geometry with 90° stereo angle, very often in a double-sided detector, is used, like in the LEP and B-Factory detectors. For higher particle densities where more than one particle might strike a detector on the average, small angle stereo is used, like in the ATLAS silicon tracker. For higher particle density, as encountered in high-intensity colliders very close to the beam pipe, pixel detectors are needed.

A very large number of channels characterizes pixel detectors. Their power consumption and need for cooling are a challenge, and if fast readout is required, there is a need for clever readout architecture. Several different types of pixel detectors are being used: drift detectors, CCDs, hybrid pixels, and monolithic active pixels. Because of their low-noise operation, excellent position resolution can be achieved when the charged sharing with neighboring pixels is exploited [31], [38]. Many pixels work in the "digital" mode, where the rate above a fixed threshold is counted.

A. Drift Detectors

In drift detectors, one coordinate is determined from the measured drift time and the well-known drift velocity in a uniform field. Drift detectors have been designed and built for the Star experiment at RHIC [32] and are the subject of intense research. One challenge is to prevent the drifting charge to diffuse into neighboring strips [33], [34]; the other is to allow the charge to be time marked for use in X-ray applications [35].

B. CCD Detectors

The development of CCD detectors was paced by their use as photon detectors in the visible band: they have completely replaced photographic plates in astronomy applications. Like silicon strip detectors, their use is following Moore's law, with the proposed SNAP satellite[2] having over 10^9 pixels and the cost falling by many orders of magnitude over 20 years of application, with the quality improving at the same time.

In HEP, the most advanced application of CCDs has been in the vertex detector of SLAC linear collider detector (SLD), which ultimately had 300 million channels [36]. The slow repetition rate of the SLC collider and the low trigger rate were the ideal condition for the use of CCDs, which require fairly long readout time because the charge has to be shifted across the rows and columns of pixels to the readout. Fig. 7 shows a "typical" picture of a Z decay into three jets, tracked with the SLD CCD detector. For use in next-generation e^+e^- colliders, a faster readout scheme is being developed [37]. An intense area of research and development is the radiation hardness of CCD detectors.

C. Hybrid Pixel Detectors

Hybrid detectors use high-resistivity detectors like strip detectors, but with much reduced area. The active area of a pixel detector is on the order of $50 \times 300\ \mu\text{m}^2$ and is determined by the size of the readout chip, which is customarily bump-bonded to the surface of the detector in flip-chip fashion. Separate optimization of detector and chip technologies can proceed, and the readout is designed to be fast enough for hybrid pixels systems to be built for use at the LHC, for BTeV [38], and the next linear collider [39].

[2]See http://snap.lbl.gov/

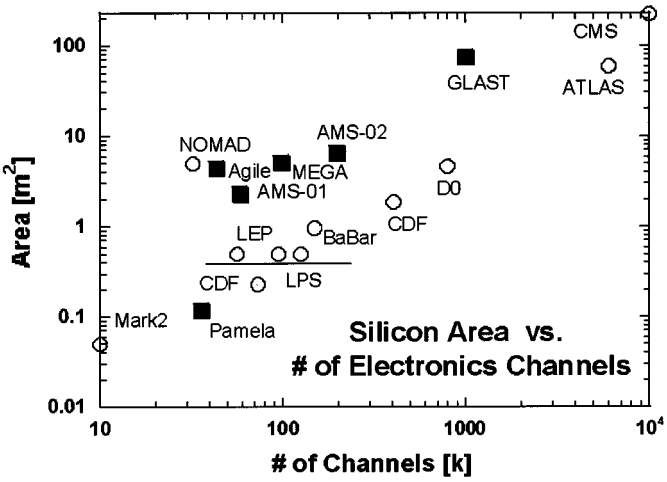

Fig. 6. The rise of the silicon detector: area of silicon detectors versus number of electronics channels. The space-based experiments (full squares) exhibit much lower channel count than their ground-based counterparts, indicating that power consumption is a severe limitation of space sciences.

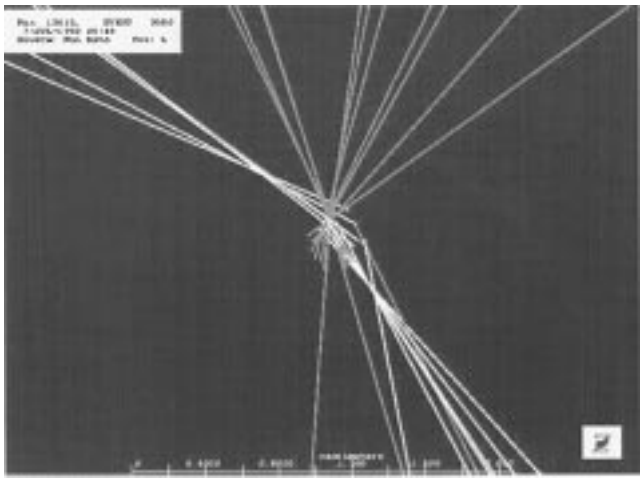

Fig. 7. "Beautiful" event picture from the 300 Mpixel SLD vertex detector. The view is along the beam line of the SLC and shows a Z decay into a gluon jet (center) and two jets containing a beauty and an antibeauty quark (right, left). The heavy quark jets show detached vertices relative to the Z decay vertex.

D. Monolithic Active Pixels

Monolithic active pixels (MAPs) [40] have grown out of the commercial application of CMOS circuits with associated photodiodes in pixel cameras. In a certain sense, a paradigm shift is occurring: the detector is integrated in the chip instead of vice-versa. Only the charge deposited in the epitaxial layer is collected by diffusion within about 150 ns. The commercial market has solved the need for low power operation. The drive of the CMOS industry to smaller feature sizes increases the radiation hardness but also decreases the thickness of the epitaxial layer. Potentially this could lead to a relative small SNR when compared with other pixel detectors.

VI. Special Trackers

Silicon detectors have found applications in many instances where reliable tracking information is needed. In an unusual application on space station Mir, a silicon detector telescope was strapped in front of Cosmonaut Adveev, who triggered readout of events when he saw the well-documented flashes that astronauts observed while in orbit. The recorded data showed a close correlation between the flash recordings and regions of increased cosmic ray flux during the orbit [41].

An application in the medical field is in nanodosimetry, where the interaction of ionizing particles with matter, here DNA, is investigated at the microscopic level [42]. Ions from the ionization process are drifted through a low-pressure area and are recorded. In this setup, the direction of the incoming and outgoing proton tracks is recorded in silicon detectors, and because the proton energy is low, the energy loss in the silicon detector allows measurement of the proton momentum (see Fig. 1).

Silicon strip detectors are used for alignment of larger detector elements. One group uses semitransparent silicon strip detectors in a laser beam and achieves submicrometer resolution [43].

VII. Photon Detection

For photons as for charged particles, the determination of the direction is crucial. In addition, in most cases, an energy determination is needed. The energy loss of photons is highly energy dependent, and there are three distinct interactions with the medium, which determine how much of the photon's directional information is retained in the detection. This is shown in Fig. 8, where the photon attenuation coefficient for Si is shown as a function of the energy [10]–[12]. The attenuation coefficient is somewhat dependent on the material: higher Z materials exhibit larger cross sections and the curves in Fig. 8 are shifted to higher energy. Three distinct regions are evident: at lower energy, the photoelectric effect is dominant, with the cross section changing by five orders of magnitude. No directional information is available in the detection of photons, and external devices like a lens, mirror, collimator, coded mask, and "proximity focus" are needed to determine the direction of the photons. In the 0.1–10 MeV region, the Compton effect allows partial reconstruction of the direction. At high energy, pair production retains the directional information of the gamma. At that point, the absorption coefficient is 7/9 of the radiation length X_o, i.e., in one radiation length of material, 54% of the gammas are converted.

VIII. X-Ray Imaging

A large part of medical imaging is in the X-ray energy range of about 20–30 keV, where tissue and bones or calcifications have very different absorption coefficients, thus making high-contrast pictures possible. The physical sizes of the objects are fairly large, proximity focusing is being applied, and silicon strips seem to be an obvious detector candidate. One of the problems with using silicon strip detectors [44] is that in the interesting energy range, the absorption length of silicon is on the order of millimeters, i.e., only a fraction of the X-rays are converted in the commonly used 300-μm-thick detectors. The other problem is that for high-rate application, double-sided detectors with crossed strips generate so-called "ghosts," i.e., wrong combinations of the two coordinates. Rotating the strip detectors by 90° can eliminate both of these problems, such that the strips are almost parallel to the X-rays, essentially forming pixels with an area of pitch times detector thickness, and the full strip length is available for the absorption. The strips are connected to an ASIC, which works in digital mode by simply counting the rate of photons, which deposit charge above a preset threshold. The X-ray tube, a collimator, and the detectors are then scanned across the object [45]. In an application using a synchrotron light source, the patient is moved across the X-ray beam [46]. The X-ray pictures show excellent contrast, and the required dose is lower when compared to conventional film use [45].

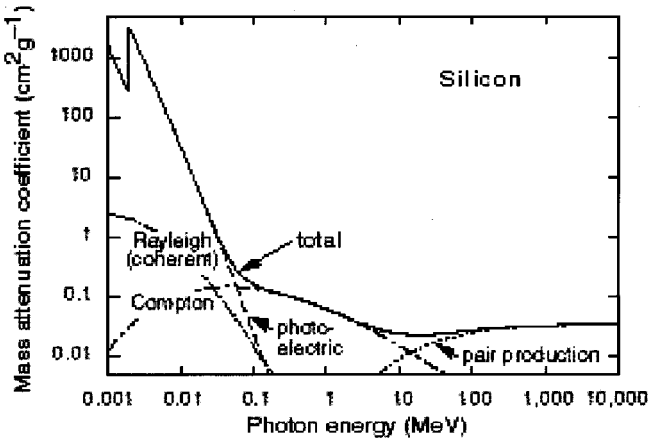

Fig. 8. Photon attenuation coefficient for Si. Three distinct regions are evident: at lower energy, the photoelectric effect is dominant, with the cross section changing by five orders of magnitude. No directional information is available here. In the 0.1–10 MeV region, the Compton effect allows partial reconstruction of the direction. At high energy, pair production retains the directional information of the gamma. From [10]–[12].

Imaging at 30 keV is being reported with a silicon detector of 300-μm thickness with pixels of 170 $\times$ 170 μm^2, read out by a chip with a 15-bit pseudorandom counter. Even though the photon detection efficiency is only 20%, good contrast pictures can be obtained [47].

For X-ray crystallography at somewhat lower energy, where the photons can be efficiently absorbed within the standard thickness of silicon detectors, hybrid pixel detectors are being developed. Using a matrix of 512 fast photon counting chips assembled on 64 detectors with 200 $\times$ 200 μm^2 pixels developed for the DELPHI detector at LEP, a total area of 25 $\times$ 25 cm^2 is instrumented [48]. Very high counting rates and very high dynamic range, i.e., contrast, are possible.

An interesting alternative to the hybrid pixel detectors is the "3-D" detector [49], which replaces the silicon detector paradigm of the planar processing with a new fabrication process where the implants are in columns between the two faces of the wafer. Because the depletion voltage depends on the distance of the columns instead of the detector thickness, this approach allows one to decouple the signal size ($\sim$ to the thickness) and the

depletion voltage ($\sim$ to the square of the column distance). Obvious applications in X-ray detection and tracking in very high radiation fields will await the practicality of having to etch the many holes into the silicon bulk and fill it with p-doped poly.

IX. Compton and Pair Imaging

At photon energies above 100 keV, the directional information is preserved when the photon interacts with a single electron or nucleus. In the Compton effect, only part of the photon energy is transferred to the electron, and the original direction is either reconstructed on a cone, or, if the direction of the scattered electron is measured, on part of a cone (see Fig. 9). As proposed in [50] and [51], measuring the energy transfer to electrons in successive Compton interactions allows the direction and energy of the photon to be reconstructed accurately.

In the Compton camera, the energy transfer and the location of the scatter are detected in a silicon pad detector with self-triggered readout chip, while the direction and energy of the scattered photon are detected in a ring of calorimeters [52]. The use of the Compton effect is sometimes referred to as "electronic collimation," replacing the mechanical collimation in clinical Anger cameras.

For hard X-ray detection in astrophysics, a Compton telescope consisting of many layers of double-sided silicon detectors is being proposed [53]. Thick silicon detectors would increase the energy and direction resolution and the detection efficiency but will require very high-resistivity detectors. An 11-layer Compton telescope prototype with a active area of 18×18 cm^2 has been built as a first step toward the medium energy gamma-ray astronomy telescope [54].

At the highest photon energies, above 100 MeV, the prevalence of pair production allows the photon detection to be done by using well-established charged particle tracking: the gamma rays convert into electron-positron pairs, which are tracked in fine-grained detectors. But a subtle paradigm shift is needed: while the charged particle tracking in magnetic fields tries to minimize the amount of material in the active volume, pair conversion trackers have to introduce extra material in order to allow enough conversions to take place, leading to the *pair conversion tracker paradigm:*

1) maximize the area;
2) intersperse tracking layers with converters;
3) keep individual converters thin.

Given that the conversion rate is proportional to the amount of material, and the angular resolution is proportional to the square root of the material due to multiple scattering of the electron and positron, a careful optimization of the amount of converter material has to be done, based on the science program. A safe but expensive solution to the problem is to distribute the converters over many layers with interspersed tracking planes, which allows one to determine the directions of the charged particle pair before they multiple scatter too much.

A large pair conversion telescope for astronomical investigations is the Large Area Telescope on GLAST (shown in Fig. 10),

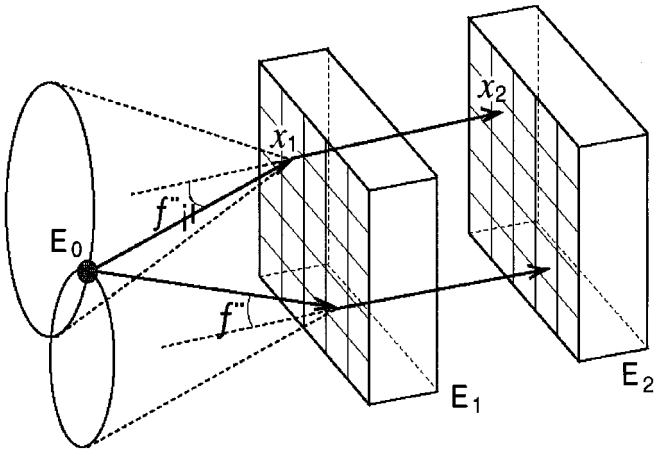

Fig. 9. Principle of Compton telescope: each measurement reconstructs the photon to be on a cone around the outgoing gamma direction. From [51].

which is being constructed to be launched in 2005 [55], [56]. It has a large area, and to minimize the schedule risk, it will be built in 16 identical "towers," each containing a silicon converter-tracker built with silicon strip detectors and a CsI hodoscopic calorimeter. The tracker will have 12 converter planes with about 3%X_o and four planes with 18%X_o converters, respectively, each followed by an x-y measurement using crossed single-sided silicon detectors. At the bottom, two additional x-y planes without converters are added for triggering on and reconstruction of conversions in the lowest converters. A prototype tower has been built and successfully tested in a beam test [57]. The final instrument will have close to 80 m^2 of silicon area and 1 million channels of ultralow-power readout electronics [58], and will need about 5 million wire bonds to assemble the wafers to ladders. The special requirements of the launch, the space environment, and the remoteness of operation have been driving the design of the tracker and detectors to be extremely simple and robust [59], [60]. With the launch of GLAST, one will be able to say that silicon detectors have arrived in space.

X. Summary

The development of silicon detectors has led to many applications in many fields, only limited by the imagination of the scientists in the field. The success of this technology can be traced to forces outside and within the science community:

Outside:

1) existence of industrial base;
2) sophistication of fabrication;
3) improvement in quality;
4) reduction in cost.

Inside:

1) maturity of designs;
2) growth of expertise;
3) improvement of assembly techniques;
4) progress in ASIC design.

At the end, real progress was made when the two communities, industry and science, started a fruitful collaboration.

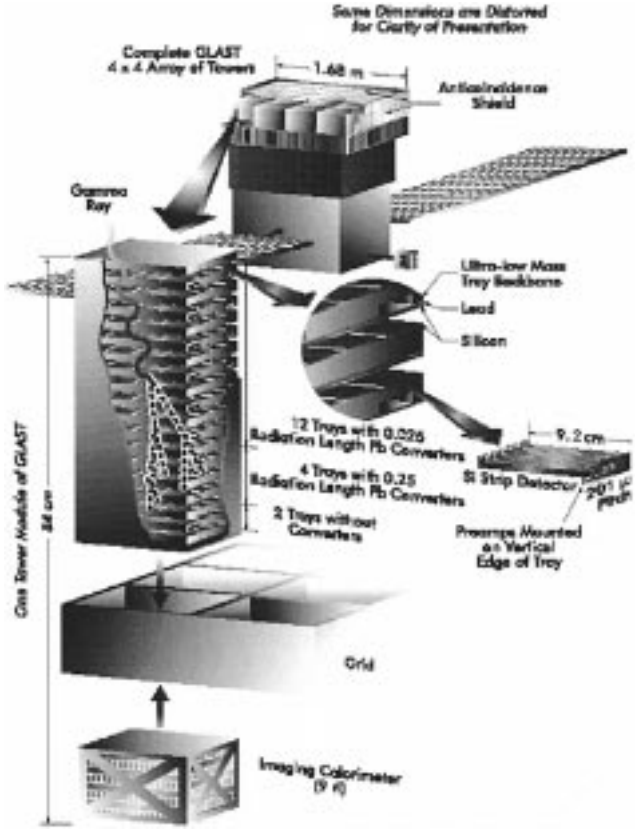

Fig. 10. Schematic view of the GLAST Large Area Telescope. The satellite based detector consists of a 4×4 array of towers, each containing silicon tracker and CSI calorimeter. The tracker towers are subdivided into 16 converter plans, each followed by silicon strip detectors with crossed strips, with two extra x-y planes at the bottom. An anticoincidence shield surrounds the whole instruments and vetoes charged particles. Photons convert in the converter foils and are tracked in the silicon layers. From [60].

ACKNOWLEDGMENT

The author would like to thank the organizers of the 2000 IEEE NSS and MIC Symposium for the informative conference. D. Groom deserves special thanks for providing Figs. 1 and 8.

REFERENCES

[1] S. M. Sze, *Physics of Semiconductor Devices*, 2nd ed. New York: Wiley, 1981.
[2] H. F.-W. Sadrozinski, "Silicon microstrip detectors in high luminosity application," *IEEE Trans. Nucl. Sci.*, vol. 45, pp. 295–302, 1998.
[3] M. Bruzzi, "Radiation damage in silicon detectors," presented at the IEEE Nuclear Science Symp., Lyon, France, Oct. 15–20, 2000.
[4] T. Dubbs, W. Kroeger, T. Nissen, T. Pulliam, D. Roberts, W. A. Rowe, H. F. W. Sadrozinski, A. Seiden, B. Thomas, A. Webster, and G. Alers, "Development of radiation-hard materials for microstrip detectors," *IEEE Trans. Nucl. Sci.*, vol. 46, pp. 839–843, 1999.
[5] W. Adam, E. Berdermann, P. Bergonzo, G. Bertuccio, F. Bogani, and E. Borchi *et al.*, "Micro-strip sensors based on CVD diamond," *Nucl. Instrum. Meth.*, vol. A453, pp. 141–148, 2000. RD42 Collaboration.
[6] G. Verzellesi, G.-F. D. Betta, and G. U. Pignatel, "Analytical model for the ohmic-side interstrip resistance of double-sided silicon microstrip detectors," presented at the IEEE Nuclear Science Symp., Lyon, France, Oct. 15–20, 2000.
[7] D. Passeri, P. Ciampolini, G. M. Bilei, M. M. Angarano, and F. Moscatelli, "Analysis and test of overhanging-metal microstrip detectors," presented at the IEEE Nuclear Science Symp., Lyon, France, Oct. 15–20, 2000.
[8] Z. Li, "Simulations of electric potential and field distributions in Si microstrip detectors with various strip widths/pitch configurations and bulk resistivities," presented at the IEEE Nuclear Science Symposium, Lyon, France, Oct. 15–20, 2000.
[9] C. Piemonte, "Simulations for the Silicon Microstrip Detector for the GLAST Experiment,", INFN Trieste Technical Report, 2000.
[10] "Review of particle physics," *Eur. Phys. J*, vol. C15, pp. 1–878, 2000.
[11] D. E. Groom, N. V. Mokhov, and S. I. Striganov, "Muon stopping power and range tables," Atomic Data Nucl. Data, submitted for publication.
[12] National Institute of Standards and Technology Physics Laboratory Physical Reference Data [Online]. Available: http://physics.nist.gov/PhysRefData/
[13] A. Sokolov, A. Loupilov, and V. Gostilo, "Recent results in development of Si(Li) peltier cooled detectors," presented at the IEEE Nuclear Science Symp., Lyon, France, Oct. 15–20, 2000.
[14] H. Kume, H. Onabe, M. Obinata, and T. Kashiwagi, "Evaluation of Si(Li) detectors by a combination of the copper staining method and X-ray analytical microscopy," presented at the IEEE Nuclear Science Symp., Lyon, France, Oct. 15–20, 2000.
[15] J. Kemmer, "Fabrication of a low-noise silicon radiation detector by the planar process," *Nucl. Instrum. Meth.*, vol. A169, p. 499, 1980.
[16] J. Kemmer, E. Belau, R. Klanner, G. Lutz, and B. Hyams, "Development of 10 um resolution silicon counters for charm signature observation with the ACCMOR spectrometer," in *Proc. Silicon Detectors for High Energy Physics*, 1981, pp. 195–217.
[17] E. Engels, S. Mani, T. Manns, D. Plants, P. F. Shepard, and J. A. Thompson *et al.*, "A silicon microstrip vertex detector for direct photon physics," *Nucl. Instrum. Meth.*, vol. A253, pp. 523–529, 1987. E706 Collaboration.
[18] J. T. Walker, S. Parker, B. Hyams, and S. L. Shapiro, "Development of high density readout for silicon strip detectors," *Nucl. Instrum. Meth.*, vol. A226, p. 200, 1984.
[19] C. Adolphsen, R. Jacobsen, V. Luth, G. Gratta, L. Labarga, A. Litke, A. Schwarz, M. Turala, C. Zaccardelli, A. Breakstone, C. J. Kenney, S. I. Parker, B. A. Barnett, P. Dauncey, D. Drewer, and J. A. J. Matthews, "The Mark-II silicon strip vertex detector," *Nucl. Instrum. Meth.*, vol. A313, pp. 63–102, 1992.
[20] A. S. Schwarz, "Silicon strip vertex detectors at LEP," *Nucl. Instrum. Meth.*, vol. A342, pp. 218–232, 1994.
[21] E. Barberis, N. Cartiglia, J. DeWitt, D. E. Dorfan, T. Dubbs, and A. Grillo *et al.*, "Design, testing and performance of the LPS readout electronics," *Nucl. Instrum. Meth.*, vol. A342, pp. 218–232, 1994.
[22] T. Kawasaki, M. Hazumi, J. Kaneko, D. Marlow, Z. Natkaniec, and H. Tajima *et al.*, "Performance of the BELLE silicon vertex detector," presented at the IEEE Nuclear Science Symp., Lyon, France, Oct. 15–20, 2000.
[23] G. Batignani, "Performances and running experience of the BaBar silicon vertex tracker," presented at the IEEE Nuclear Science Symp., Lyon, France, Oct. 15–20, 2000.
[24] M. Pauluzzi, "The construction of the AMS silicon tracker," presented at the Vertex 2000, July 2000.
[25] F. Filthaut, "Production and testing of the D0 silicon microstrip tracker," presented at the IEEE Nuclear Science Symp., Lyon, France, Oct. 15–20, 2000.
[26] R. Brenner, "The ATLAS semiconductor tracker," *Nucl. Instrum. Meth.*, vol. A446, pp. 243–254, 2001.
[27] S. Perriès, "The CMS central tracker," presented at the IEEE Nuclear Science Symp., Lyon, France, Oct. 15–20, 2000.
[28] P. Bloch, A. Peisert, A. Cheremukhin, I. Golutvin, N. Zamiatin, S. Golubkov, N. Egorov, Y. Kozlov, and A. Sidorov, "Investigation of silicon sensors quality as a function of the ohmic side processing technology," presented at the IEEE Nuclear Science Symp., Lyon, France, Oct. 15–20, 2000.
[29] G. E. Moore, "Cramming more components onto integrated circuits," *Electronic*, Apr. 19, 1965.
[30] E. do Couto e Silva, "The assembly of the silicon tracker of the beam test engineering model of the GLAST beam test engineering model," *Nucl. Instrum. Meth.*, vol. A446, pp. 376–382, 2001.
[31] M. S. Passmore, R. Bates, K. Mathieson, V. O'Shea, M. Rahman, P. Seller, and K. Smith, "Charge sharing effects in pixellated photon counting detectors," presented at the IEEE Nuclear Science Symp., Lyon, France, Oct. 15–20, 2000.
[32] D. Lynn, "The star silicon drift detector vertex tracker," presented at the IEEE Nuclear Science Symp., Lyon, France, Oct. 15–20, 2000.
[33] A. Castoldi, C. Guazzoni, and L. Strueder, "Silicon drift detectors with spiraling electron transport and reduced lateral broadening," presented at the IEEE Nuclear Science Symp., Lyon, France, Oct. 15–20, 2000.

[34] J. Sonsky, R. W. Hollander, P. M. Sarro, and C. W. E. van Eijk, "Multi-anode sawtooth SDD for X-ray spectroscopy fabricated on NTD wafers," presented at the IEEE Nuclear Science Symp., Lyon, France, Oct. 15–20, 2000.

[35] A. Castoldi, C. Guazzoni, L. Strueder, and P. Rehak, "Spectroscopic-grade X-ray imaging up to 100 kHz frame rate with controlled drift detectors," presented at the IEEE Nuclear Science Symp., Lyon, France, Oct. 15–20, 2000.

[36] C. J. S. Damerell, "Charge-Coupled Devices as Particle Tracking Detectors,", RSI 69, 1998.

[37] T. Greenshaw and D. Milstead, "A CCD vertex detector for the future linear collider," presented at the IEEE Nuclear Science Symp., Lyon, France, Oct. 15–20, 2000.

[38] S. Kwan, "Beam test results of the BTeV silicon pixel detectors," presented at the IEEE Nuclear Science Symp., Lyon, France, Oct. 15–20, 2000.

[39] M. Battaglia, S. Borghi, M. Caccia, R. Campagnolo, W. Kucewicz, H. Palka, and A. Zalewska, "Hybrid pixel detector development for the linear collider vertex tracker," presented at the IEEE Nuclear Science Symp., Lyon, France, Oct. 15–20, 2000.

[40] J. D. Berst, G. Claus, C. Colledani, G. Deptuch, W. Dulinski, U. Goerlach, Y. Hu, D. Husson, G. Orazi, R. Turchetta, J. L. Riester, and M. Winter, "Design and testing of a monolithic active pixel sensor for charged particle tracking," presented at the IEEE Nuclear Science Symp., Lyon, France, Oct. 15–20, 2000.

[41] V. Bidoli, M. Casolino, M. P. De Pascale, G. Furano, A. Morselli, and L. Narici *et al.*, "Study of cosmic rays and light flashes on board space station Mir, the Sileye experiment," *Adv. Space Res.*, vol. 25, no. 10, pp. 2075–2079, 2000.

[42] S. Schemelinin, A. Breskin, R. Chechik, P. Colautti, and R. Schulte, "First ionization cluster measurements on the DNA scale in a wall-less sensitive volume," *Radiat. Prot. Dosim.*, vol. 82, pp. 43–50, 1999.

[43] M. F. Garcia, S. Horvath, H. Kroha, A. Ostapchuk, and S. Schael, "Semi-transparent silicon strip sensors for the precision alignment of tracking detectors," presented at the IEEE Nuclear Science Symp., Lyon, France, Oct. 15–20, 2000.

[44] A. Papanestis, G. Iles, E. Corrin, M. Raymond, G. Hall, F. Triantis, N. Manthos, I. Evangelou, P. vd Stelt, T. Tarrant, R. Speller, and G. Royle, "A radiographic imaging system based upon a 2-D silicon microstrip sensor," presented at the IEEE Nuclear Science Symp., Lyon, France, Oct. 15–20, 2000.

[45] M. Lundqvist, B. Cederström, V. Chmill, M. Danielsson, and B. Hasegawa, "Evaluation of a photon counting X-ray imaging system," presented at the IEEE Nuclear Science Symp., Lyon, France, Oct. 15–20, 2000.

[46] M. Prest, "FROST, a low-noise high-rate photon counting ASIC for X-ray application," presented at the 8th Pisa Meeting Advanced Detectors, La Bidola, Elba, Italy, May 2000.

[47] S. R. Amendolia, M. G. Bisogni, U. Bottigli, A. Ceccopieri, P. Delogu, and G. Dipasquale *et al.*, "Comparison of imaging and spectrometric performances for different semiconductors detectors," presented at the IEEE Nuclear Science Symp., Lyon, France, Oct. 15–20, 2000.

[48] P. Delpierre, J. F. Berar, L. Blanquart, B. Caillot, J. C. Clemens, and C. Mouget, "X-ray pixel detector for crystallography," presented at the IEEE Nuclear Science Symp., Lyon, France, Oct. 15–20, 2000.

[49] C. Kenney, S. Parker, B. Krieger, and B. Ludewigt, "3D architecture silicon sensors: Test results: Future plans," presented at the IEEE Nuclear Science Symp., Lyon, France, Oct. 15–20, 2000.

[50] T. Kamae, R. Enomoto, and N. Hanada, "A new method to measure energy, direction and polarization of gamma rays," *Nucl. Instrum. Meth.*, vol. A260, pp. 254–267, 1987.

[51] Y. F. Yang, Y. Gono, S. Motomura, S. Enomoto, and Y. Yano, "A compton camera for multi-tracer imaging," presented at the IEEE Nuclear Science Symp., Lyon, France, Oct. 15–20, 2000.

[52] D. Meier, A. Czermak, P. Jalocha, B. Sowicki, W. Dulinski, and G. Maehlum *et al.*, "Silicon detector for a compton camera in medical imaging," presented at the IEEE Nuclear Science Symp., Lyon, France, Oct. 15–20, 2000.

[53] R. A. Kroeger, W. N. Johnson, J. D. Kurfess, B. F. Phlips, and E. A. Wulf, "Gamma ray energy measurement using the multiple compton technique," presented at the IEEE Nuclear Science Symp., Lyon, France, Oct. 15–20, 2000.

[54] F. Schopper, R. Andritschke, G. Kanbach, J. Kemmer, M.-O. Lampert, P. Lechner, R. Richter, P. Rohr, V. Schönfelder, L. Strueder, and A. Zoglauer, "Development of silicon strip detectors for a medium energy gamma telescope," presented at the IEEE Nuclear Science Symp., Lyon, France, Oct. 15–20, 2000.

[55] P. Michelson (PI), *GLAST LAT*: Stanford Univ., 1999. Response to AO 99-OSS-03.

[56] Proposal for GLAST, , E. D. Bloom, Ed., 1998. SLAC-R-522.

[57] E. Atwood, W. Atwood, B. Bhatnager, E. Bloom, J. Broeder, and V. Chen *et al.*, "The silicon tracker of the beam test engineering model of the GLAST large-area telescope," *Nucl. Instrum. Meth.*, vol. A457, pp. 126–136, 2001.

[58] R. P. Johnson, P. Poplevin, H. F.-W. Sadrozinski, and E. Spencer, "An amplifier-discriminator chip for the GLAST silicon-strip tracker," *IEEE Trans. Nucl. Sci.*, vol. 45, pp. 927–932, 1998.

[59] H. F.-W. Sadrozinski, "Radiation issues in the gamma-ray large area space telescope GLAST," presented at the F2k, the 3rd Florence Symp. Radiation Hardness, Florence, Italy, June 28–30, 2000.

[60] ——, "GLAST, a gamma-ray large area space telescope," *Nucl. Instrum. Meth.*, vol. A446, pp. 292–299, 2001.